Condensed Matter Physics.
Physics of nanostructures.
Mesoscopic structures

UDC 535.5

EDN LFAWTO
https://www.doi.org/10.33910/2687-153X-2024-5-1-3-9

Three-photon absorption and photoluminescence in films of liquid-crystal polymers with embedded CdSe/ZnS quantum dots

V. Yu. Nesterov [1, 2], N. D. Presnov [1], S. V. Zabotnov [1], A. S. Merekalov [3], O. N. Karpov [1, 3], G. A. Shandryuk [1, 3], R. V. Talroze [1, 3], L. A. Golovan [✉1]

[1] Lomonosov Moscow State University, 1–2 Leninskie Gory, Moscow 119991, Russia
[2] Moscow Institute of Physics and Technology, 9 Institutsky Lane, Moscow 141701, Russian Federation
[3] A. V. Topchiev Institute of Petrochemical Synthesis, Russian Academy of Sciences, 29 Leninsky Ave., Moscow 119991, Russia

Authors

Vyacheslav Yu. Nesterov, e-mail: nesterovvy@my.msu.ru

Nikita D. Presnov, e-mail: presnovnikita@yandex.ru

Stanislav V. Zabotnov, ORCID: 0000-0002-2528-4869, e-mail: zabotnov@physics.msu.ru

Alexey S. Merekalov, ORCID: 0000-0002-8996-9568, e-mail: alexis@ips.ac.ru

Oleg N. Karpov, ORCID: 0000-0002-7314-7885, e-mail: o-karpov777@mail.ru

Georgiy A. Shandryuk, ORCID: 0000-0003-4349-5296, e-mail: shandgo@mail.ru

Raisa V. Talroze, ORCID: 0000-0002-9151-5493, e-mail: rtalroze@ips.ac.ru

Leonid A. Golovan, ORCID: 0000-0002-6838-5395, e-mail: golovan@physics.msu.ru

For citation: Nesterov, V. Yu., Presnov, N. D., Zabotnov, S. V., Merekalov, A. S., Karpov, O. N., Shandryuk, G. A., Talroze, R. V., Golovan, L. A. (2024) Three-photon absorption and photoluminescence in films of liquid-crystal polymers with embedded CdSe/ZnS quantum dots. *Physics of Complex Systems*, 5 (1), 3–9. https://www.doi.org/10.33910/2687-153X-2024-5-1-3-9 EDN LFAWTO

Received 8 December 2023; reviewed 10 January 2024; accepted 10 January 2024.

Funding: This work was supported by Russian Science Foundation project No. 23-19-00246, https://rscf.ru/project/23-19-00246/

Abstract. In this paper, we studied nonlinear absorption of infrared (IR) (1250 nm) femtosecond pulses and visible photoluminescence (PL) excited by them in liquid-crystal (LC) polymer films with embedded CdSe/ZnS core-shell type quantum dots (QDs). The dependence of nonlinear transmission on incident intensity indicated three-photon absorption in the films, with the three-photon absorption coefficient for the QD-LC polymer composite comparable with the one for bulk CdSe. The spectrum of PL excited by IR pulses coincides with one-photon excited PL spectrum. Dependence of the PL signal on the IR laser radiation power is cubic with further saturation for the spectral region from 2.10 to 2.25 eV, with saturation intensity decreasing with lower PL photon energy. The presence of the second-harmonic signal in the up-conversion spectrum results in its variation with an excitation power increase.

Keywords: semiconductor quantum dots, liquid-crystal polymer, up-conversion, photoluminescence, multiphoton absorption

Introduction

Nowadays, there is no need to prove the prospects of semiconductor quantum dots (QDs) or their applications in various fields. Strong restriction in charge carrier movements in the semiconductor nanoparticle significantly changes its electronic and optical properties (Efros, Brus 2021), opening up various ways of their usage in optoelectronics (Litvin et al. 2017), photovoltaics (Kirmani et al. 2020), laser generation (Jung et al. 2021), biomedical applications (Le et al. 2023), etc.

We should mention the use of the semiconductor QDs for up-conversion, i. e., light emission with wavelength below the excitation wavelength, among their highly promising applications (Rakovich, Donegan 2008). Up-conversion could be used for optical cooling (Ye et al. 2021), laser generation (Moon et al. 2021), infrared (IR) radiation detection (Zhou et al. 2020), bioimaging (Chen, Liang 2014) and therapy (Dutta, Barik 2022). Various mechanisms are responsible for up-converted PL, including population of defect states, phonon-assisted PL, two- and three-photon absorption (Laktaev et al. 2022; Wang et al. 2023), etc.

For many practical applications it would be useful to have a composite of semiconductor QDs and a transparent matrix that immobilizes them. Moreover, to ensure a maximal PL signal of the composite, QD concentration should be rather high, and ordered arrays of QDs should be formed. This can be done in a liquid-crystal (LC) polymer. When incorporated into the smectic LC structure, CdSe QDs break hydrogen bonds in the polymer, forming ionic bonds between polymeric carboxyl groups and QD surfaces, and nanolayers of QDs chemically bonded to the side chains of the macromolecules (Shandryuk et al. 2008). QD-polymer composites can contain up to 60 wt. % of QDs and demonstrate rather effective PL (Golovan et al. 2020; Tselikov et al. 2015). Transmission electron microscopy (TEM) data provides evidence of uniform QD distribution in composites (Shandryuk et al. 2008).

In this paper, we report on up-conversion in CdSe/ZnS core-shell QDs in a LC polymer and discuss the mechanism involved.

Experimental techniques

Samples

We used CdSe/ZnS core-shell QDs since they have more efficient PL and, in contrast to core-type CdSe QDs, core-shell QDs demonstrate mainly excitonic PL whereas the defect PL band is strongly suppressed (Golovan et al. 2020). The QDs were synthesized by means of a single-step synthetic method which helps to form a core/shell structure with a chemical composition gradient (Bae et al. 2008). The QDs were placed in a side chain acrylic LC polymer poly[4-(ω-acryloyloxyhexyloxy)benzoic acid] (BA-6PA). The QDs are built into a smectic layer with the thickness determined by the QD diameter. The structure of the initial LC polymer is retained for the QD fraction in the composite below a certain value (Shandryuk et al. 2008). The average diameter of the QDs is 4.8 nm with a standard deviation of 0.8 nm. A detailed description of the synthesis of QDs and LC polymer and the formation of composite films can be found elsewhere (Golovan et al. 2020). In our study we used 15-μm thick BA-6PA LC polymer films with embedded CdSe/ZnS QDs (20 and 40 wt. % concentration) and CdSe/ZnS QD suspension in toluene.

Optical measurements

Excitation of up-converted PL (UCPL) was carried out by radiation of a Cr:forsterite laser (Avesta-Project, Ltd, 1250 nm wavelength, 80 fs pulse duration, 1 nJ pulse energy, 80 MHz repetition rate). The radiation was focused on the film or in a cuvette with the QD suspension with a short-focus lens (focal length 7.5 mm, numerical aperture 0.3); the same lens was used to collect the PL signal, which was recorded with a Princeton Instrument Spectra Pro 2500i spectrometer equipped with a CCD array. UCPL spectra were compared with PL spectra excited by the second harmonic of radiation of a Nd:YAG laser EKPLA 2143A (532nm wavelength, 25 ns pulse duration, 10 Hz repetition rate) with photon energy over the QD bandgap. Laser radiation intensity at the samples in both cases did not exceed 10 GW/cm^2. Transmitting the excitation radiation through a gradient filter allowed it to be varied, which was used in obtaining dependences of the PL signals on the excitation intensity. The same short-focus lens and gradient filter were also used in a nonlinear-transmission measurement. Signals of IR radiation chopped at frequency 715 Hz incident on and transmitted through the LC polymer film with embedded 40 wt. % concentration of the QDs were detected by two diodes FD-10G and registered by two lock-in voltmeters SR 830.

 https://www.doi.org/10.33910/2687-153X-2024-5-1-3-9

Results and discussion

The PL spectra excited by IR femtosecond radiation in the composites containing 20 and 40 wt. % of the QDs and in the QD suspension in toluene are shown in Fig. 1. The PL spectra width is explained by QD size distribution. One can see a red shift of the PL spectra with an increase in QD concentration.

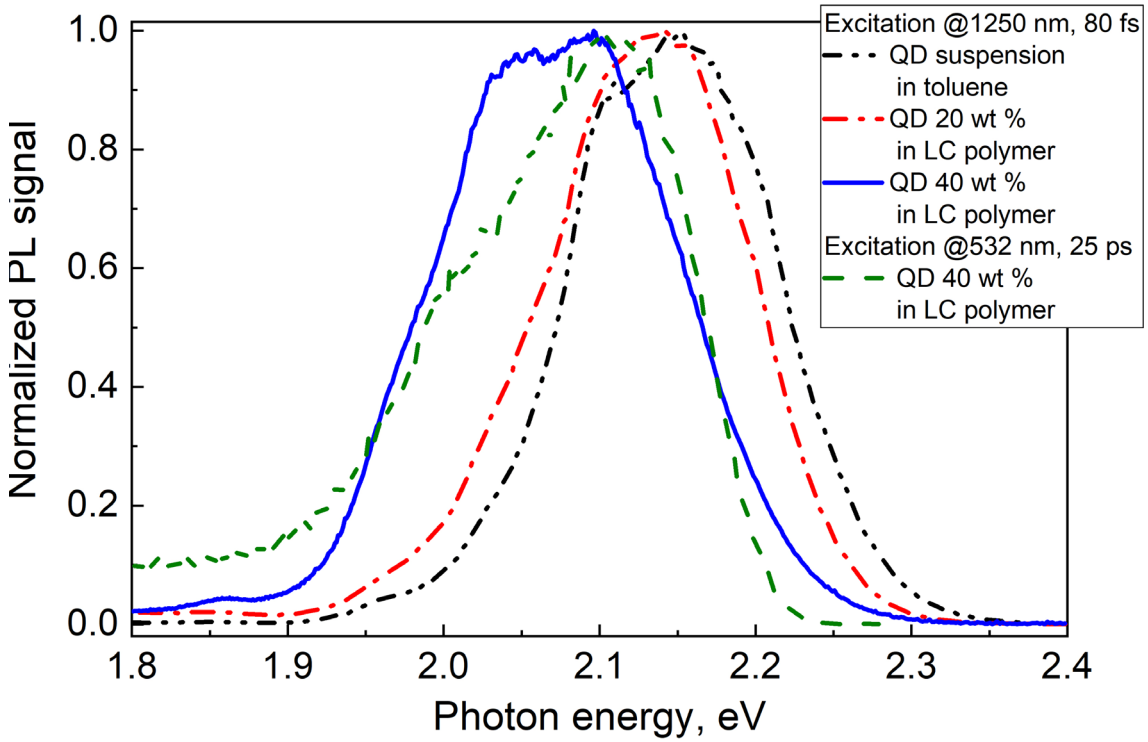

Fig. 1. Normalized PL spectra for the composites containing 20 wt. % (dot-dash line) and 40 wt. % (solid line) of the QDs and the QD suspension in toluene (dot-dot-dash) excited by IR femtosecond pulses and for PL spectra excited by picosecond laser radiation at wavelength of 532 nm (dash line)

The effect can be explained by an energy transfer from smaller QDs to bigger QDs, which emits photons of less energy due to their smaller band gaps. The PL spectra excited by femtosecond pulses at 1250 nm and by picosecond pulses at 532 nm are very close. It is worth noting that the PL spectra are not excited by continuous-wave laser radiation at 1250 nm and the same and even higher average power, which shows that PL emission depends on excitation radiation intensity, not power.

The UCPL spectrum strongly depends on focusing the IR laser beam at the surface of the sample (Fig. 2). We should mention that for the used laser beam the waist radius w_0 is 6 μm and Rayleigh length (distance where the beam section is twice the size at the waist) $\pi w_0^2 / \lambda$, where λ is wavelength, is 90 μm, which significantly exceeds the film thickness. The maximal PL signal is achieved when the laser beam waist is at the film surface, as confirmed by the maximum of the third-harmonic signal. Further displacement of the beam focal region inside the sample results in a UCPL signal decrease and red shift of its maximum. These facts can be explained by the reabsorption of the PL emitted inside the film.

To establish the UCPL mechanism, it would be instructive to study specific properties of laser radiation absorption by the films of the LC polymer with embedded QDs and obtain a dependence of the PL spectra on excitation power.

An experiment on the femtosecond IR pulse transmission through the LC polymer film with 40 wt. % concentration of the QDs demonstrates a transmittance decrease with an incident radiation intensity increase (Fig. 3, inset). The PL photon energy can exceeds the excitation photon energy more than twice, which is why three-photon absorption can be supposed to excite UCPL. Indeed, in the simplest case of the only three-photon absorption in the medium, transmission of intensity I along the coordinate z inside the medium is governed by the equation:

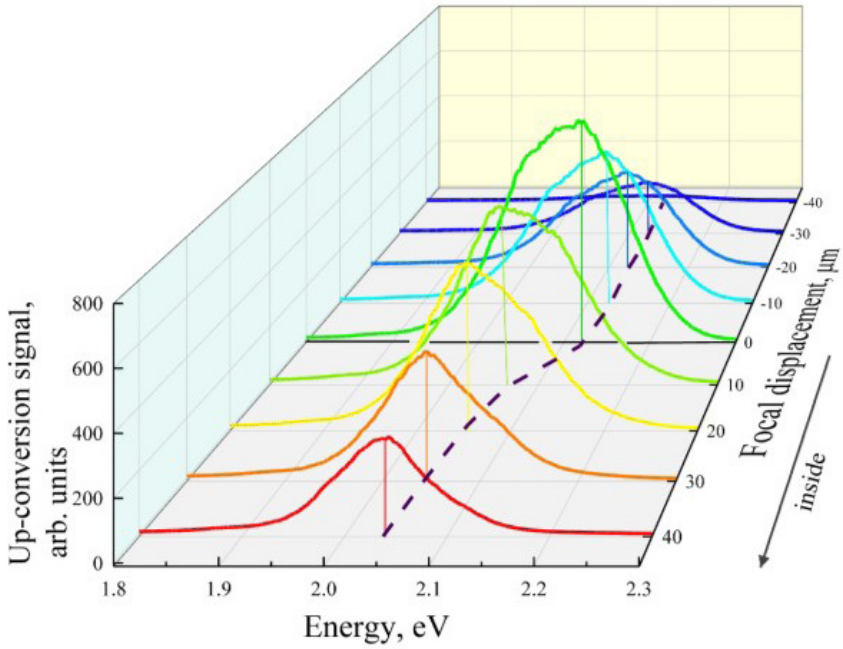

Fig. 2. Variation of the UCPL spectrum with the movement of the excitation beam focus

$$\frac{dI}{dz} = -\gamma I^3 \ , \tag{1}$$

where γ is a three-photon absorption coefficient. From Eq. 1 one can conclude the following ratio:

$$\frac{T_0^{\,2}}{T^2} = 1 + 2\gamma d I_0^{\,2} \ , \tag{1}$$

where d is film thickness, I_0 is intensity of incident radiation, T is transmittance at intensity I_0, while T_0 is film transmittance at very low radiation intensity.

Fig. 3 presents the obtained dependence of the $T_0^{\,2}/T^2$ value on $I_0^{\,2}$. Nonlinear absorption effects are noticeable for intensity above 10 MW/cm^2, and Eq. 2 is in line with experimental data. This allows us to estimate the three-photon absorption coefficient γ, which was found to be equal to 0.17 cm^3/W^2. Although the QD volume fraction in the composite film is about 0.09, the γ value obtained for it is comparable with the one for bulk semiconductors (0.13–0.24 cm^3/W^2 @ 1.54 μm for CdSe and 0.0017 cm^3/W^2 @ 1.06 μm for ZnS (Benis et al. 2020)). Thus, we can conclude that UCPL is caused by the three-photon absorption of the IR femtosecond radiation.

The dependence of the UCPL signal on laser radiation power would also be very instructive. The PL signal excited by radiation at wavelength of 532 nm shows linear dependence on the laser radiation power. For the used intensities it does not demonstrate any significant saturation.

Fig. 4 presents UCPL spectra of the QD suspension in toluene and QDs embedded into the LC polymer with a concentration of 40 wt. % obtained at different average excitation radiation power P_{exc}. In the latter case, one can see a significant UCPL spectrum variation with an increase of the excitation radiation power (Fig. 4c), whereas for the QD suspension in toluene variations are much less pronounced (Fig. 4a).

This fact makes it necessary to follow changes of a separate spectral component of the UCPL signal (1.95, 2.00, 2.05, 2.10, 2.15, 2.20 and 2.25 eV) with excitation power variations. For more clarity, we normalize them by the ones for lower power intensity (15 mW for the QD toluene suspension and 7 mW for the composite of QDs and LC polymer) (Figs. 4b, 4d). As one can see, these dependences are very close for both media. UCPL signals in the spectral region from 2.10 to 2.25 eV demonstrate cubic dependence on the P_{exc} value below 50 mW (intensity of 7 GW/cm^2); for higher excitation power the UCPL signal tends towards saturation. Saturation of the UCPL signal at 2.05 eV starts at a much lower P_{exc} value (20 mW). This fact could be due to an energy transfer from smaller QDs with a higher band gap to bigger

 https://www.doi.org/10.33910/2687-153X-2024-5-1-3-9

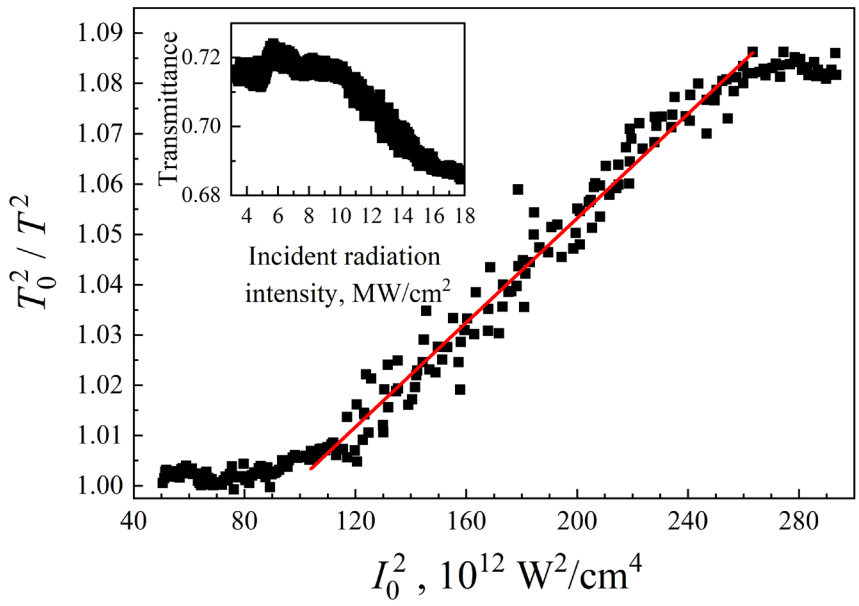

Fig. 3. T_0^2/T^2 vs. I_0^2. The line is an approximation of dependence according to Eq. 2. The inset is dependence of the LC film with embedded QDs (40 wt. %) transmittance on intensity of incident femtosecond pulses at wavelength of 1250 nm

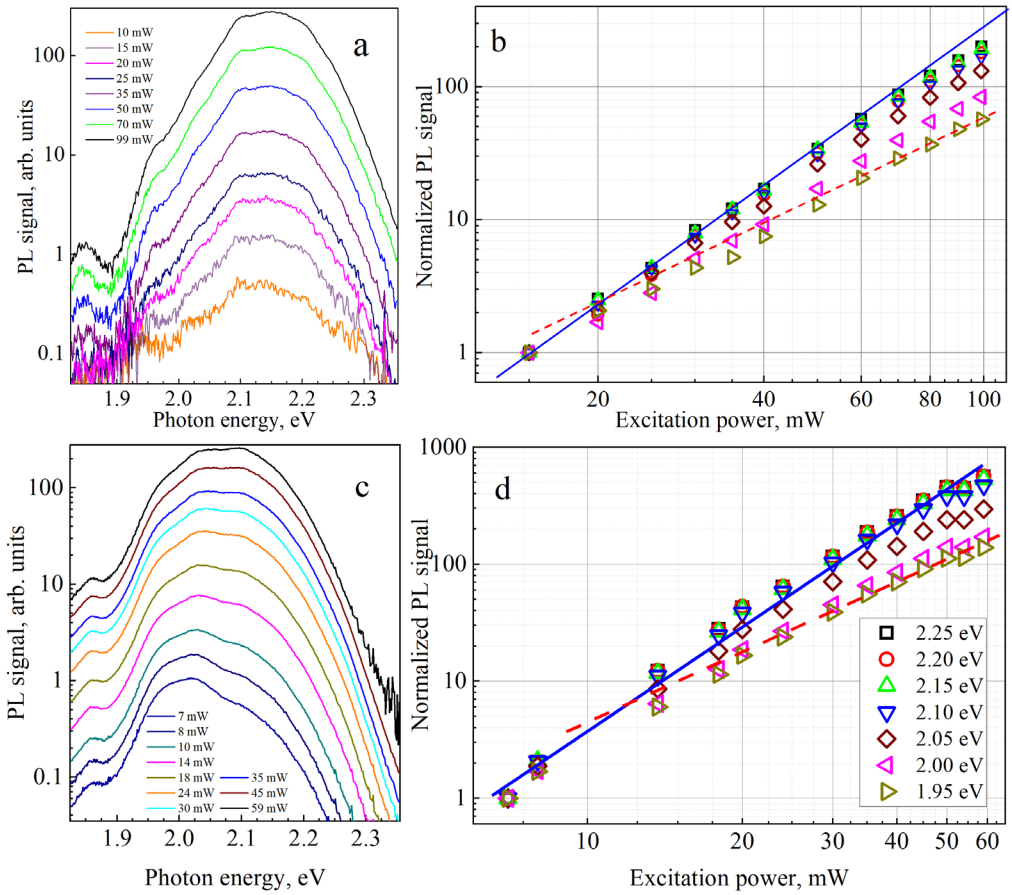

Fig. 4. UCPL spectra for the QD suspension in toluene (a) and QDs embedded into the LC polymer (40 wt. %) (c) and dependences of UCPL spectral components at different photon energies normalized by spectral components taken for the same photon energy at P_{exc} = 15 mW for the QD suspension in toluene (b) and by spectral components at P_{exc} = 7 mW for the QDs embedded into the LC polymer (40 wt. %) (d) on average excitation radiation power. Solid and dashed lines correspond to the cubic and quadratic dependences of the UCPL signal on P_{exc}

QDs with a lower band gap. At least, the UCPL spectral components in the region 1.95 to 2.00 eV demonstrate their quadratic dependence on P_{exc} for the excitation power above 20 mW. It is worth noting that this spectral range corresponds to the second-harmonic generated by the Cr:forsterite laser radiation. Thus, we can conclude that a part of the UCPL spectrum for QDs embedded into the LC polymer is the second harmonic spectrum generated in QDs, which results in variation of the UCPL spectrum with variations of the excitation power. Since the concentration of the QDs in the suspension is obviously lower than in the LC polymer-QD composite, the second-harmonic spectrum is less pronounced in the former medium.

Conclusions

We demonstrated that the up-conversion signal generated both in a suspension of CdSe/ZnS quantum dots in toluene and in a composite film of quantum dots and a liquid-crystal polymer under excitation by femtosecond infrared (1250 nm) pulses is caused by three-photon absorption. A nonlinear transmission measurement allowed us to find the three-photon absorption coefficient for the LC polymer composite with 40 wt. % QD concentration, with the value comparable to the one for bulk CdSe. The dependence of the up-conversion signal in the spectral range 2.10 to 2.25 eV on the average excitation radiation power is cubic and tends towards saturation, whereas for the spectral range 1.95 to 2.00 eV, which is the region of the second harmonic of the excitation radiation, the up-converted signal demonstrates quadratic dependence on the excitation radiation power. As a result, in a composite film with rather high QD concentration, the up-conversion spectrum varies with excitation variation.

Conflict of Interest

The authors declare that there is no conflict of interest, either existing or potential.

Author Contributions

The authors have made an equal contribution to the paper.

References

Bae, W. K., Char, K., Hur, H., Lee, S. (2008) Single-step synthesis of quantum dots with chemical composition gradients. *Chemistry of Materials*, 20 (2), 531–539. https://doi.org/10.1021/cm070754d (In English)

Benis, S., Cirloganu, C., Cox, N. et al. (2020) Three-photon absorption spectra and bandgap scaling in direct-gap semiconductors. *Optica*, 7 (8), 888–899. https://doi.org/10.1364/OPTICA.396056 (In English)

Chen, Y., Liang, H. (2014) Applications of quantum dots with upconverting luminescence in bioimaging. *Journal of Photochemistry and Photobiology B: Biology*, 135, 23–32. https://doi.org/10.1016/j.jphotobiol.2014.04.003 (In English)

Dutta, R., Barik, P. (2022) Upconversion and downconversion quantum dots for biomedical and therapeutic applications. In: P. Barik, S. Monal (eds.). *Application of quantum dots in biology and medicine. Recent advances*. Singapore: Springer Publ., pp. 229–263. https://doi.org/10.1007/978-981-19-3144-4_12 (In English)

Efros, A. L., Brus, L. E. (2021) Nanocrystal quantum dots: From discovery to modern development. *ACS Nano*, 15 (4), 6192–6210. https://doi.org/10.1021/acsnano.1c01399 (In English)

Golovan, L. A., Elopov, A. V., Zaitsev, V. B. et al. (2020) Photoluminescence of CdSe and CdSe/ZnS quantum dots in amorphous and liquid-crystalline polymer matrices. *Polymer Science. Series A: Physics*, 62 (6), 701–713. http://dx.doi.org/10.1134/S0965545X20060048 (In English)

Jung, H., Ahn, N., Klimov, V. I. (2021) Prospects and challenges of colloidal quantum dot laser diodes. *Nature Photonics*, 15 (9), 643–655. https://doi.org/10.1038/s41566-021-00827-6 (In English)

Kirmani, A. R., Luther, J. M., Abolhasani, M., Amassian, A. (2020) Colloidal quantum dot photovoltaics: Current progress and path to gigawatt scale enabled by smart manufacturing. *ACS Energy Lett*ers, 5 (9), 3069–3100. https://doi.org/10.1021/acsenergylett.0c01453 (In English)

Laktaev, I. D., Saidzhonov, B. M., Vasiliev, R. B. et al. (2022) Two-photon excited biexciton photoluminescence in colloidal nanoplatelets CdSe/CdS. *Journal of Luminescence*, 252, article 119414. https://doi.org/10.1016/j.jlumin.2022.119414 (In English)

Le, N., Kim, K. (2023) Current advances in the biomedical applications of quantum dots: Promises and challenges. *International Journal of Molecular Science*, 24 (16), article 12682. https://doi.org/10.3390/ijms241612682 (In English)

Litvin, A. P., Martynenko, I. V., Purcell-Milton, F. et al. (2017) Colloidal quantum dots for optoelectronics. *Journal of Material Chemistry A*, 5 (26), 13252–13275. https://doi.org/10.1039/C7TA02076G (In English)

Moon, B.-S., Lee, T. K., Jeon, W. C. et al. (2021) Continuous-wave upconversion lasing with a sub-10 W cm^{-2} threshold enabled by atomic disorder in the host matrix. *Nature Communications*, 12 (1), article 4437. https://doi.org/10.1038/s41467-021-24751-z (In English)

Rakovich, Yu. P., Donegan, J. F. (2008) Anti-Stokes photoluminescence in semiconductor nanocrystal quantum dots. In: A. L. Rogach (ed.). *Semiconductor nanocrystal quantum dots*. Vienna: Springer Publ., pp. 257–275. http://dx.doi.org/10.1007/978-3-211-75237-1_9 (In English)

Shandryuk, G. A., Matukhina, E. V., Vasil'ev, R. B. et al. (2008) Effect of H-bonded liquid crystal polymers on CdSe quantum dot alignment within nanocomposite. *Macromolecules*, 41 (6), 2178–2185. http://dx.doi.org/10.1021/ma701983y (In English)

Tselikov, G. I., Timoshenko, V. Yu., Golovan, L. A. et al. (2015) Role of the polymer matrix on the photoluminescence of embedded CdSe quantum dots. *ChemPhysChem*, 16 (5), 1071–1078. http://dx.doi.org/10.1002/cphc.201402913 (In English)

Wang, F., He, M., Huang, B. et al. (2023) Band gap engineering improves three-photon luminescence of quantum dots for deep brain imaging. *Analytical Chemistry*, 95 (29), 10947–10956. https://doi.org/10.1021/acs.analchem.3c00845 (In English)

Ye, Z., Lin, X., Wang, N. et al. (2021) Phonon-assisted up-conversion photoluminescence of quantum dots. *Nature Communications*, 12 (1), article 4283. https://doi.org/10.1038/s41467-021-24560-4 (In English)

Zhou, W., Shang, Y., García de Arquer, F. P. et al. (2020) Solution-processed upconversion photodetectors based on quantum dots. *Nature Electronics*, 3 (5), 251–258. https://doi.org/10.1038/s41928-020-0388-x (In English)